JOURNAL OF MATERIALS SCIENCE 16 (1981) 973–982

The role of amorphous phase separation in crystal nucleation in splat cooled Li_2O-SiO_2 glasses

E. D. ZANOTTO*
Departamento de Engenharia de Materiais, Universidade Federal de São Carlos, São Carlos, São Paulo, Brazil

A. F. CRAIEVICH
Departamento de Física e Ciência dos Materiais, Instituto de Física e Química de São Carlos, Universidade de São Paulo, São Carlos, São Paulo, Brazil

Amorphous phase separation and its influence on crystal nucleation in Li_2O-SiO_2 splat cooled glasses was studied. By means of small-angle X-ray scattering and optical reflection microscopy associated with stereological analysis it was shown that the crystal nucleation rate is increased during the early stages of primary and secondary phase separation. These observations emphasize the important role played by the diffusion zone around the amorphous droplets acting as nucleation sites. Some suggestions are advanced to explain why some authors found that the amorphous separation does not influence the crystal nucleation.

1. Introduction

Since Stookey's patent in 1956 [1], glass-ceramic materials have been intensively studied due to their interesting properties and applications. An important step in the formation of glass ceramics is crystal nucleation. It is known that a large increase in the nucleation rate can be obtained by adding nucleating agents. However the precise effect of the amorphous phase separation, which precedes crystallization in several glass-ceramics, on crystal nucleation is still uncertain. For example, Vogel and Gerth [2] and Ohlberg *et al.* [3] have suggested that the existence of interfaces in the phase-separated glasses could enhance crystal nucleation. Cahn [4] and Uhlmann [5] suggested that local changes in composition due to phase separation can increase or decrease the thermodynamic driving force for crystallization. Uhlmann [5] also suggested that: (i) the separation can result in one of the liquid phases having higher atomic mobility in the range of larger undercoolings than the parent homogeneous phase, and (ii) the interfacial regions between the separated phases may be enriched in some component, providing a locally larger driving force for nucleation or a locally higher atomic mobility. Recently, Ramsden [6] in a detailed study, showed that the amorphous phase separation exerts a pronounced effect on the crystal nucleation kinetics in $BaO-SiO_2$ glasses with 25 to 30 mol% BaO. The progressive shift in the composition of the Ba-rich matrix phase with time caused changes in the thermodynamic driving force and in the kinetic barrier to nucleation which in turn caused a marked increase in the nucleation rate. The study of the nucleation kinetics in relation to quantitative data on the morphology of the two liquid phases showed no evidence of heterogeneous nucleation at the liquid–liquid interfaces.

Studying glasses in the Li_2O-SiO_2 system, Nakagawa and Izumitani [7] observed that the difference in the number of crystals formed in the liquid–liquid phase-separated glass (29.0 mol% Li_2O) and in the quenched (homogeneous) glass

*Present address: Department of Ceramics, Glasses and Polymers, The University of Sheffield, UK.

0022–2461/81/040973–10$03.00/0

was negligible. They also found that the maximum nucleation rate of the $Li_2O{\cdot}2SiO_2$ crystals was at 480° C while that of the amorphous droplets was at 450° C. They concluded that the two phenomena are independent. Harper *et al.* [8], studying 70 mol % SiO_2–30 mol % Li_2O and 69 mol % SiO_2–30 mol % Li_2O–1 mol % P_2O_5 glasses, contended that amorphous phase separation did not promote crystal nucleation but could affect it indirectly by influenzing the crystal growth rate. Tomozawa [9] utilized small-angle X-ray scattering (SAXS) and transmission optical microscopy to study Li_2O–SiO_2 glasses and observed a large increase in the crystal nucleation rate in a 29.5 mol % Li_2O glass when it was undergoing phase separation. He pointed out that in the early stages of phase separation the silica-rich minor phase consisted of droplets with diffusion zones (silica depleted zones) at their interfaces, and proposed that these zones could act as favourable sites for the heterogeneous nucleation of crystals. Matusita and Tashiro [10] using 25 mol % Li_2O–75 mol % SiO_2 and 33 mol % Li_2O–66.7 mol % SiO_2 compositions with addition of various oxides have found evidence for an increased nucleation rate induced by phase separation. Recently, Hautojarvi and Komppa [11] studied Li_2O–SiO_2 glasses with positron life-time and annihilation line-shape measurements and showed that phase separation increased the density of crystal nuclei and the rate of volume crystallization.

Thus, although numerous experiments have been performed, the effects of amorphous phase separation on crystal nucleation and growth have by no means been clearly established. The influence of phase separation may be specific to certain glass systems. Theoretically, amorphous phase separation should influence crystal nucleation in one or more ways according to the points discussed by Uhlmann [5]. In practice it is difficult to determine which mechanism is involved.

Therefore, more work is needed to clarify the subject, and the present study follows the approach used by Tomozawa [9]. Glass samples of the Li_2O–SiO_2 system obtained by splat cooling have been studied. This technique was employed to minimize the probability of occurrence of amorphous phase separation and crystal nucleation during cooling from the melt. The thin specimens obtained by means of this technique are suitable for SAXS measurements. Reflection optical microscopy, associated with stereological analysis, was also employed. We believe that this technique is more reliable than the transmission optical microscopy method, where errors due to overlap of crystals in the thin section may occur.

2. Theory

2.1. Small-angle X-ray scattering

The SAXS technique is very useful in studying sub-microscopic composition heterogeneities. In particular, by means of the integral of SAXS intensity in reciprocal space it is possible to determine whether the separation occurs at an early stage, e.g. nucleation and growth, or if it occurs at a more advanced stage, when the larger segregation zones grow at the expense of the smaller ones, i.e. the coarsening stage.

The integrated SAXS intensity in reciprocal space, Q, for an isotropic system is [12]

$$Q = 4\pi \int I(s)s^2 \mathrm{d}s, \qquad (1)$$

where s is the modulus of the scattering vector in reciprocal space. By definition, $s = 2 \sin \theta/\lambda$, where θ is half the scattering angle, ϵ, and λ is the wavelength of the incident X-ray beam. If the scattering is concentrated at small angles the relationship between ϵ and s can be approximated by $s = \epsilon/\lambda$. The integral Q is related to the structural parameters of the analysed system by [9]

$$Q = \text{constant}\,[V_1 V_2 (C_1 - C_2)^2], \qquad (2)$$

where V_1 and V_2 are the volume fractions of the separated particles and matrix respectively and C_1 and C_2 the compositions of these phases. If Q becomes constant after a certain period of isothermal treatment, the amorphous separation is in the coarsening stage since, in that case, the compositions and volume fractions of the separated phases are constant.

Guinier [12] has shown that the SAXS intensity scattered at sufficiently small angles by a system containing a low concentration N of random particles is given by

$$I(s) = N(\rho - \rho_0)^2 \exp(-\tfrac{4}{3}\pi^2 R_0^2 s^2), \qquad (3)$$

where $(\rho - \rho_0)^2$ is the difference between the electronic densities of the particles and matrix and R_0 is the radius of gyration of the particles.

At larger angles Equation 3 is no longer valid. The SAXS intensity in the limit of large scattering angles may be represented by Porod's law [13]

$$I(s) = \left[\frac{(\rho - \rho_0)^2}{8\pi^3}\right]\left(\frac{S'}{s^4}\right), \quad (4)$$

where S' is the total interfacial area. This assumes a "two-phase" system in which the particles and matrix have uniform electronic densities, the particles have well-defined interfaces and are randomly oriented with any shape except that of a needle or plate.

Equations 1 and 4 can be applied to analyse experimental SAXS curves obtained using pinhole collimation.

2.2. The classical nucleation theory

According to classical theory [14] the steady-state nucleation rate, I, may be expressed as a function of temperature T by

$$I = A \exp\left[-(W^* + \Delta G_D)/kT\right], \quad (5)$$

where A is a constant, approximately independent of temperature, W^* and ΔG_D are the thermodynamic and kinetic free energy barriers to nucleation, respectively, and k is Boltzmann's constant.

For one component systems, the kinetic barrier ΔG_D can be related to the viscosity, η, of the liquid by means of the Stokes–Einstein relation [15] so that Equation 5 becomes

$$I = \left(\frac{A'}{\eta}\right) \exp\left(-W^*/kT\right), \quad (6)$$

where A' is a constant.

2.3. Stereological analysis

The numbers of particles per unit area that intersect a planar section (micrograph), N_A, can be related to the number of particles per unit volume, N_v, by means of the De Hoff and Rhines [16] relations for particles with a constant prolate ellipsoidal shape, i.e.

$$N_v = \frac{2N_A\bar{Z}}{\pi k(q)}, \quad (7)$$

where $\bar{Z}$ is the average of the reciprocal of minor axes of the planar intersections on the micrograph and $k(q)$ is a function of the shape of the particles which may be evaluated through the graphs supplied by De Hoff and Rhines. Equation 7 allows the number of crystals per unit volume to be determined from reflection optical micrographs. The method is described in detail by James [17].

3. Experimental procedure

Three compositions were melted in Pt crucibles in a SiC furnace at 1450 ± 10° C for 2 h, quenched in water, and crushed and remelted for an additional 2 h to ensure homogeneity. The batch materials utilized were Brazilian quartz and laboratory grade Li_2CO_3. Samples were prepared by the splat cooling technique using a device which has been described by Craievich [18]. The samples obtained were plates 0.25 mm thick, ready for SAXS analysis.

The nominal compositions were 29.0, 31.0 and 33.3 mol% Li_2O. According to the phase diagram (Fig. 1) the 29.0 and 31.0 compositions should phase separate whereas the 33.3 composition should not, for the heat treatments used. This was confirmed by SAXS and replica electron microscopy. Some loss of Li_2O probably occurred during melting. From previous literature the maximum loss might be as high as 1 mol%. However, from the position of the phase boundary, such a shift in composition would not be likely to cause the glass with 33.3 mol% Li_2O to separate, and no phase separation was detected in this glass. The total iron content in all the glasses was 0.11 wt% of Fe_2O_3 by analysis. On melting, all the glass samples were clear and bubble-free.

The thermal treatments to induce phase separation and crystal nucleation were carried out in a tubular furnace at 440, 450, 475 and 500 ± 1° C for different periods of time. The same samples were heat treated at 600 ± 10° C for 15 min or 580 ± 10° C for 20 min in order to grow the crystalline nuclei formed at the lower nucleation temperature to a sufficient size to be observed in an optical microscope. These growth temperatures were chosen with the requirements that both the nucleation of new crystals and the dissolution of the existing ones were negligible [17]. All samples reached the quoted temperatures in 2 to 3 min. The fast heating rate was employed in order to minimize the nucleation of amorphous particles or crystals during heating.

In order to obtain optical micrographs, the samples with a double stage heat treatment were polished with SiC grit and colloidal Ce_2O_3 and etched with a 2% HF solution for 2 min. Micrographs of heat-treated samples were similar to those shown by James [17] and Tomozawa [9]. The crystal morphologies were also fully discussed by these authors.

Approximately 300 crystalline particles were counted and measured in each sample to obtain the parameters N_A and $\bar{Z}$ of Equation 7. A reason-

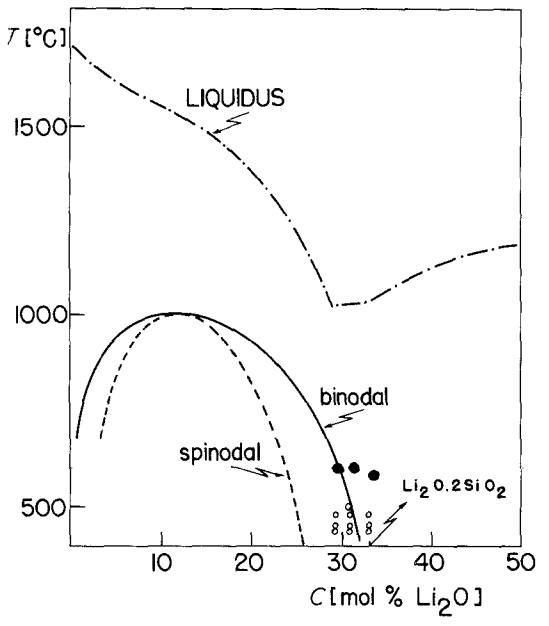

Figure 1 Miscibility gap in the Li_2O–SiO_2 system according to the literature [9] showing the location of the nucleation (○) and growth (●) heat treatments employed (nominal glass compositions).

able estimate for the statistical error in N_v was ± 10%.

The SAXS curves were obtained using a Rigaku X-ray generator and goniometer, scintillation counter and a specially-designed step scanning device [19]. The experimental curves were corrected for parasitic scattering and electronic background and were normalized to an equivalent sample thickness and equivalent incident X-ray beam intensity.

The cross-section of the X-ray beam was "linear and infinite" [20] and the SAXS intensities were obtained in relative units. Under these experimental conditions Equation 1 can be written as

$$Q = \text{constant} \int F(\epsilon)\epsilon \, d\epsilon, \qquad (8)$$

where $F(\epsilon)$ is the normalized SAXS intensity.

The angular dependence of SAXS intensity at very small angles remains the same for "linear and infinite" collimation. Hence Equation 3 can be written

$$F(\epsilon) = \text{constant} \exp\left(-\frac{4\pi^2}{3\lambda^2} R_0^2 \epsilon^2\right). \qquad (9)$$

At larger angles, where Equation 4 is valid for point-like collimation, the angular dependence of the SAXS intensity for "linear and infinite" collimation is given by

$$F(\epsilon) = \text{constant}/\epsilon^3. \qquad (10)$$

The mathematical treatment of SAXS data (corrections and normalization) and statistical errors were carried out by means of a PDP 11/45 computer.

4. Results

4.1. Phase separation (SAXS)

The series of normalized SAXS curves for samples of the 31.0 mol% Li_2O glass heat treated at 475° C (inside the miscibility gap) are plotted in Fig. 2. The experimental SAXS curves were determined for $\epsilon_m < \epsilon < \epsilon_M$, the limits being imposed by experimental factors (high parasitic scattering for $\epsilon < \epsilon_m$ and too low scattering intensity for $\epsilon > \epsilon_M$). In order to obtain the integral Q of Equation 8 $F(\epsilon)$ was determined for $\epsilon < \epsilon_m$ by using Guinier's equation and for $\epsilon > \epsilon_M$ by means of Porod's equation.

Fig. 3 shows that the behaviour predicted by Equation 9 is followed in a wide angular domain with some deviation at very small angles, near $\epsilon = 0.2°$. This was found to be due to the contribution of surface roughness of the samples. A detailed study of the surface contribution to SAXS from glasses will be published elsewhere. In the present work a correction for the scattering from the surface was obtained by extrapolating to zero angle the experimental SAXS intensity in the angular domain where the Guinier plot was linear.

Porod's law (Equation 10) was satisfied for the 31.0 mol% Li_2O glass samples which were heat treated for periods longer than 6 h at 475° C. This is shown in Fig. 4 where the slopes of the curves $\ln F(\epsilon)$ against $\ln \epsilon$ are approximately equal to -3. This indicates that the conditions stated in Section 3.1 are satisfied except in the early stages, and enables the curves to be extrapolated for $\epsilon > \epsilon_M$.

The deviations of some of the SAXS curves from Porod's equation were expected because the hypothesis of a system of two phases each with a uniform electronic density is not satisfied during the early stages. However, when the separation is in a more advanced stage and the depleted zones around the droplets have sizes much larger than the droplets, the samples behave approximately like a two-density system.

From the experimental SAXS intensities and the extrapolations described above, values of the integral Q of Equation 8 were obtained.

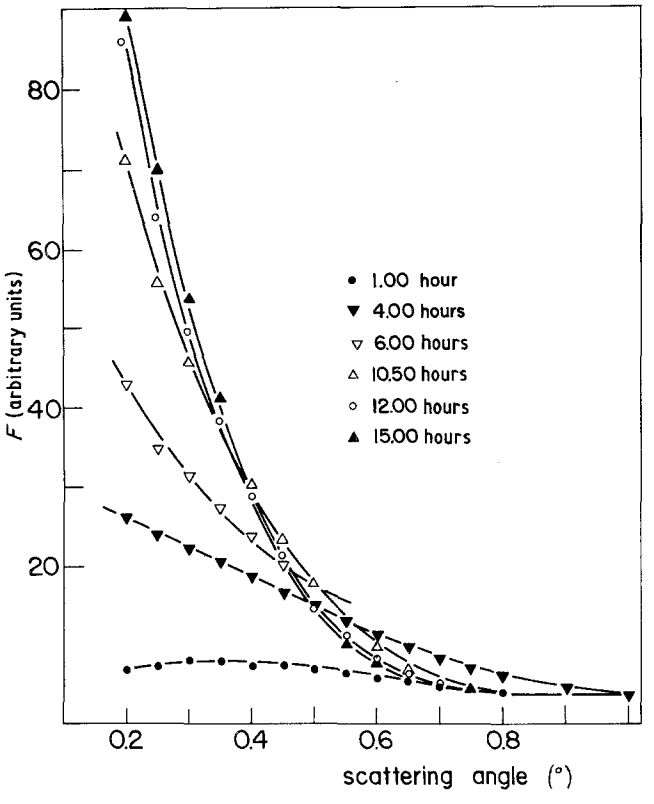

Figure 2 SAXS curves of 31.0 mol% Li_2O glass samples heat treated at 475° C for different periods.

The evolution of Q with the isothermal heat treatment is shown in Fig. 5 for the 31.0 mol% Li_2O glass samples heat treated at 475° C. It can be observed that initially Q increases with time but after about 15 h reaches a constant value. This shows that the amorphous separation is in a pure coarsening stage after approximately 15 h at 475° C. However, it should be emphasized that coarsening begins before 15 h.

4.2. Crystal nucleation

4.2.1. Effect of the different stages of phase separation on crystal nucleation

Samples of the 31.0 mol% Li_2O and 33.3 mol% Li_2O glasses were given a nucleation heat treatment first at 475° C and later at 600° C for 15 min (31.0 mol% Li_2O) and 580° C for 20 min (33.3 mol% Li_2O).

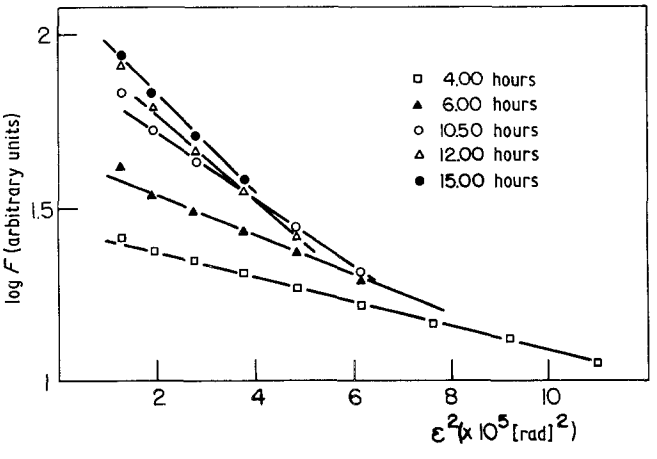

Figure 3 Guinier plots of 31.0 mol% Li_2O glass samples heat treated at 475° C.

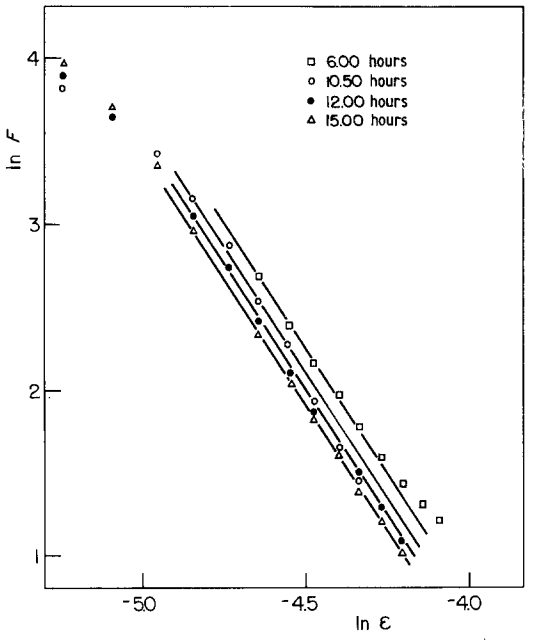

Figure 4 Porod plots of 31.0 mol% Li_2O glasses heat treated at 475° C.

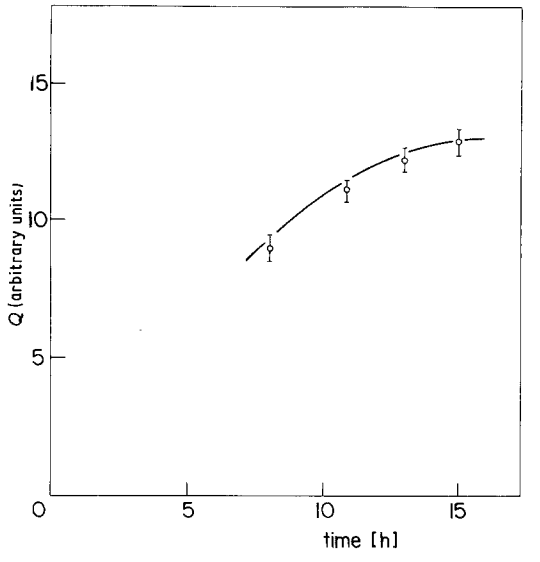

Figure 5 SAXS integrals of 31.0 mol% Li_2O glass samples heat treated at 475° C.

In Fig. 6 the crystal nucleation curves are plotted against the time of heat treatment for the 31.0 mol% Li_2O glass in which phase separation occurred simultaneously with crystal nucleation, and also for the 33.3 mol% Li_2O glass in which no phase separation occurred. During the first 10 h the slope of the N_v (t) curve for the heterogeneous glass is clearly greater than that of the homogeneous one. Fig. 5 shows that the amorphous phase separation in the 31.0 mol% Li_2O glass is in the nucleation and growth stage during that period. There also appears to be a decrease in the slope dN_v/dt (the nucleation rate) as the phase separation approaches the coarsening stage, although further experimental results would be needed to confirm this.

In order to check the influence of the coarsening stage of liquid–liquid immiscibility of the nucleation of crystals, some specimens of the 31 mol% Li_2O glass were heat treated first at 500° C for 4 h and then subjected to the double heat treatment at 475 and 600° C. Tomozawa's SAXS studies confirm that after heat treating 31.0 mol% Li_2O glass samples for 4 h at 500° C, the amorphous phase separation is in the coarsening stage.

Fig. 7 shows that the crystal nucleation rates, dN_v/dt, for the fully phase-separated glass are approximately equal to those for the homogeneous glass during the first 4 h of heat treatment at 475° C. After 4 h dN_v/dt for the former glass begins to increase gradually. It is clear that some structural rearrangement is occurring. This point will be discussed later.

The present results are compared with those of Tomozawa [9] and James [18] for glasses with compositions close to 33.3 mol% in Fig. 8 and for glasses containing 31.0 mol% Li_2O in Fig. 9. These results were obtained using essentially the same nucleation temperature (475 or 476° C). It is clear that the nucleation rate is constant with time for the 33.3 mol% Li_2O glasses but there are some differences in the values for different authors. The large number of crystals shown in Tomozawa's plot is probably due to nucleation during cooling from the melt or heating to the

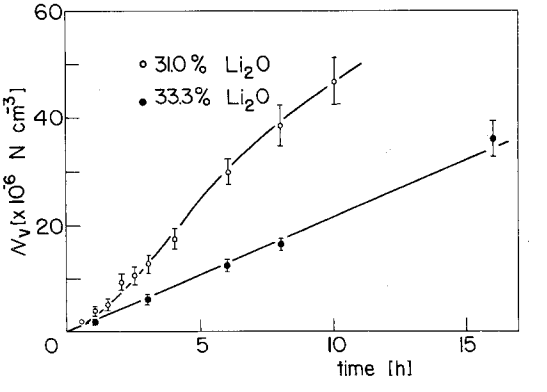

Figure 6 Crystal nucleation curves of phase separated (31.0 mol% Li_2O) and homogeneous (33.3 mol% Li_2O) glasses nucleated at 475° C.

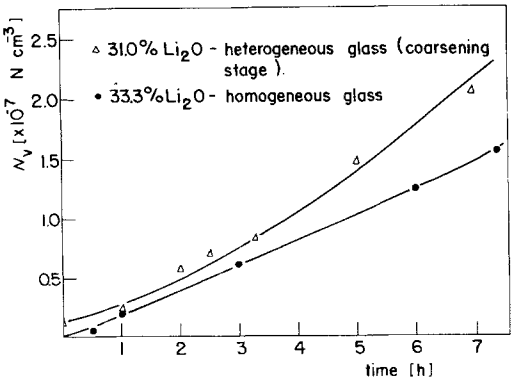

Figure 7 Crystal nucleation curves of a 31.0 mol% Li_2O glass first heat treated at 500° C for 4 h and then at 475° C, and of a 33.3 mol% Li_2O glass nucleated at 475° C.

nucleation and growth temperatures. The presence of minor batch impurities and dissolved Pt from the crucible has negligible effect on the nucleation rates of Li_2O–SiO_2 glasses, as shown by James *et al.* [21]. The differences in slopes of the three curves of Fig. 8 may be due to different water contents in the glasses, as shown by Gonzalez–Oliver *et al.* [22]. Another possibility is that there are small differences in the base compositions of the glasses, some of them having compositions nearer the stoichiometric composition (33.3 mol% Li_2O, 66.7 mol% SiO_2) than the others. From Fig. 9 it can be seen that the pronounced curvature found by Tomozawa for his 31.0 mol% Li_2O glass was not observed in the present work. Again this may be due to a small difference in

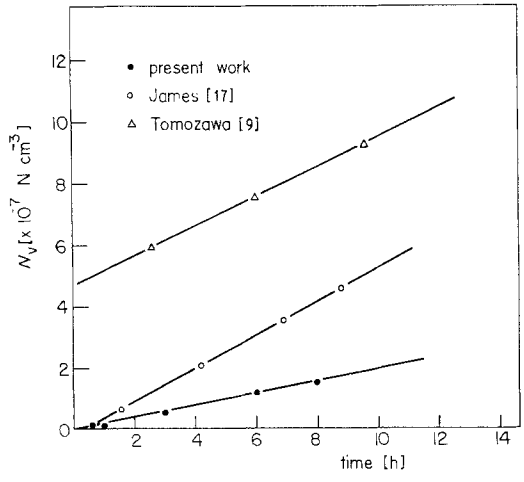

Figure 8 Crystal nucleation curves of nominally 33.3 mol% Li_2O glasses from Tomozawa [9] and present work (nucleation temperature 475° C), and from James [18] (nucleation temperature 476° C).

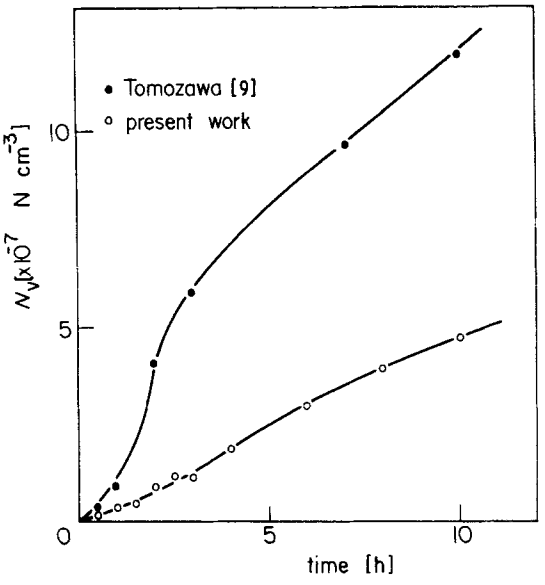

Figure 9 Crystal nucleation curves of nominally 31.0 mol% Li_2O glasses nucleated at 475° C, from Tomozawa [9] and present work.

overall composition between the glasses. However, the present results and those of Tomozawa agree in one important respect, i.e. the glass that phase separated shows a significantly higher nucleation rate than the glass which does not undergo phase separation.

4.2.2. Effect of the volume fractions of the amorphous phases

To detect the effects of the volume fractions of the separated amorphous phases on the crystal nucleation, samples with 29.0, 31.0 and 33.3 mol% Li_2O were nucleated at 475° C for 8 h and then subjected to the growth heat treatment. Also other samples were nucleated at 440 and 450° C for 8 h. This long period of nucleation treatment was employed in order to minimize the effects of non-steady state nucleation, which is principally observed at low nucleation temperatures.

Curves of number of nuclei per unit volume (N_v) against composition are shown in Fig. 10. The location of the immiscibility boundary (binodal) is also depicted. All the curves show a maximum at approximately 31.0 mol% Li_2O.

In Fig. 11 the "apparent nucleation rates" for a sample with 29.0 mol% Li_2O, heat treated for 8 h at different temperatures, are plotted. In the same figure is plotted the curve obtained by Nakagawa and Izumitani [7] showing the number of the amorphous droplets in a 29.0 mol% Li_2O glass as a function of temperature. The interesting

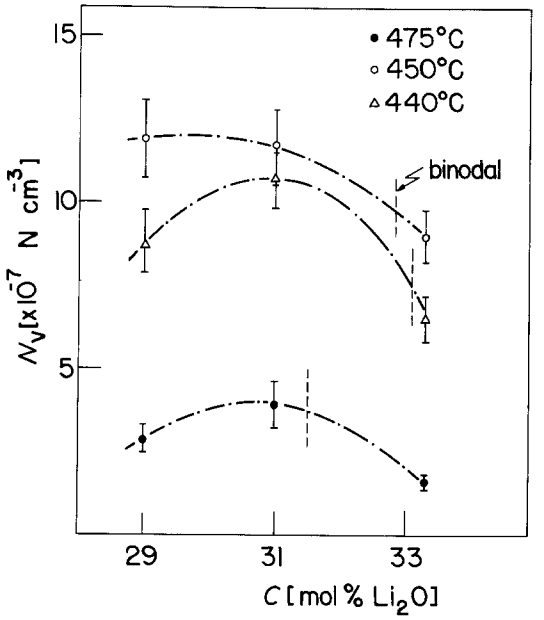

Figure 10 Number of crystals per unit volume of Li_2O–SiO_2 glasses heat treated for 8 h at different temperatures (nominal compositions).

point is the good agreement in the temperature of maximum nucleation rate (approximately 450° C) for both amorphous separation and crystal nucleation. This agreement also suggests that there may be a relationship between the two phenomena.

5. Discussion

According to classical nucleation theory the crystal nucleation rate of the 33.3 mol% Li_2O glass should be greater than that of the 29.0 and 31.0 mol% Li_2O glasses because the composition of the former is close to the stoichiometric composition of the crystalline phase $Li_2O{\cdot}2SiO_2$ even allowing for some loss of lithia during melting. Thus, W^* and the viscosity will be smaller for the 33.3 mol% Li_2O glass. This should cause dN_v/dt of the 29.0 and 31.0 mol% Li_2O glasses to be smaller (Equation 6). The expected behaviour was not observed experimentally and Figs 6 and 9 show clearly that amorphous separation increases the crystal nucleation rate.

The observed small increase of the crystal nucleation rate in the glass fully separated at 500° C, and later heat treated 4 h at 475° C (Fig. 7), suggests that "secondary phase separation" is occurring in the amorphous matrix (Fig. 12). The nucleation and growth stage of the secondary phase separation could be responsible for this increase of the crystal nucleation rate. To confirm this, further SAXS experimental work is required. However, this suggestion would be in accord with the theory of Tomozawa that SiO_2 depleted zones around the amorphous particles act as nucleation sites for the crystals. That explanation is consistent with the results of Fig. 6, since Fig. 5 shows that the increased crystal nucleation rate is observed only when the phase separation is in the nucleation and growth stage, i.e. when a diffusion profile exists around the amorphous SiO_2 droplets.

The maximum observed in Fig. 10 can be explained also by taking into account the influence of phase separation. As the composition moves towards the centre of the miscibility gap, the nucleation rate of the crystalline phase $Li_2O{\cdot}2SiO_2$ would decrease as expected through classical nucleation theory (the viscosity and W^* increase). However, the opposite effect would occur if the phase separation has an accelerating effect on crystal nucleation, due for example to the presence of diffusion zones around the droplets. These two opposing effects might level to a maximum in N_v for a particular composition, as in fact is observed in Fig. 10. The same figure may explain why some authors concluded that amorphous separation does not influence the crystal nucleation. To observe that effect it appears to be necessary to study samples with compositions

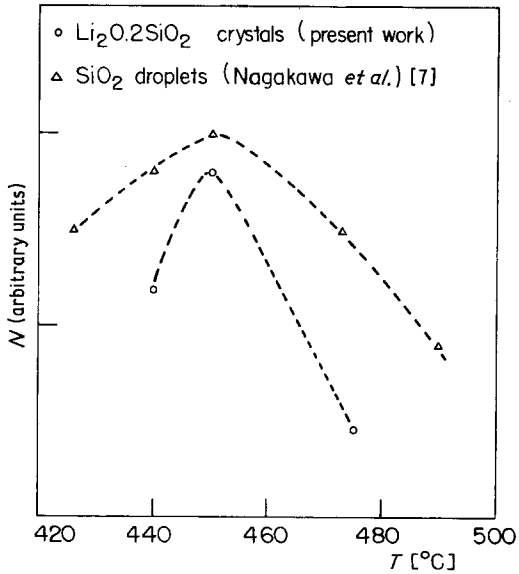

Figure 11 Number of crystals per unit volume and number of amorphous droplets per unit area of 29.0 mol% Li_2O glasses as a function of the nucleation temperature.

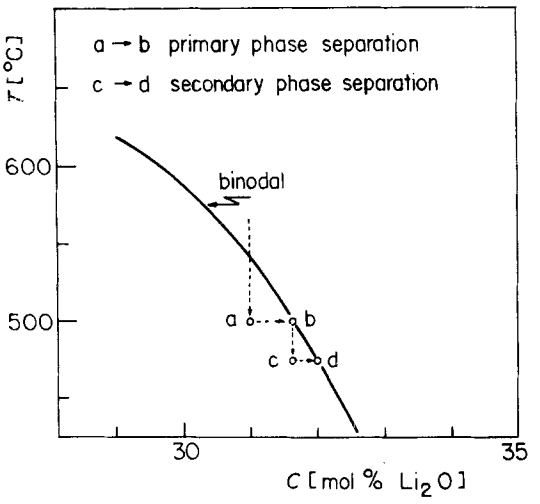

Figure 12 Schematic composition path of the matrix of samples heat treated at 500° C first and at 475° C later.

inside the binodal but not too far from the stoichiometric composition.

As stated earlier the nominal composition of the homogeneous glass is 33.3 mol% Li_2O but it was estimated that the real composition is approximately 32.3 mol% Li_2O. This can explain the greater nucleation rate, by about a factor of two and a half, shown by James' results (Fig. 8). The analysed composition of his samples is 33.1 mol% Li_2O, which is nearer the stoichiometric crystalline phase $Li_2O{\cdot}2SiO_2$. Hence, it appears that, near the stoichiometric composition, the rate of nucleation of crystals is strongly dependent on the composition.

The curves of Figs 6 and 10 show that the crystal nucleation rate, in phase separated glasses, increases by a factor of approximately two over the nominal 33.3 mol% Li_2O glass. The maximum nucleation rate is almost coincident with that observed for James' glass (33.1 mol% Li_2O). Hence, it is possible that one important role of the diffusion zones around the amorphous droplets is to bring about regions of the stoichiometric composition somewhere in the composition profiles.

While amorphous phase separation can increase the crystal nucleation rate by a factor of about two, Matusita and Tashiro [23] have shown that the addition of 3.0 mol% P_2O_5 in a 33.3 mol% Li_2O, 66.7 mol% SiO_2 glass increases the crystal nucleation by five orders of magnitude. Thus, nucleating agents have a much more pronounced effect than phase separation. Such a large influence can also mask the effect of phase separation and might explain how some authors have concluded, when studying glasses containing nucleating agents, that phase separation has no effect on crystal nucleation.

6. Conclusion

The experimental results obtained with primary and secondary phase separated Li_2O–SiO_2 glasses indicates that amorphous phase separation increases the crystal nucleation rate if there are compositional profiles around the amorphous droplets. It is suggested that the existence of regions of the stoichiometric composition (33.3 mol% Li_2O) somewhere in the diffusion profiles could be a major contribution of phase separation in increasing the crystal nucleation rate. To decide between this suggestion and the explanation proposed by Tomozawa that crystalline nuclei may form in the diffusion zones with a lowering of surface energy (heterogeneous nucleation) further experimental work is required.

Acknowledgement

The authors wish to thank the FAPESP, Brazil for partial support of this work. We also wish to thank Dr Peter F. James of the Department of Ceramics, Glasses and Polymers of the University of Sheffield, UK for helpful discussions of the main results of this research and for giving valuable suggestions in finishing the manuscript.

References

1. S. D. STOOKEY, Brit. Patent No. 752 243. (1956).
2. W. VOGEL and K. GERTH, Symposium on Nucleation and Crystallization in Glasses and Metals (American Ceramic Society, Columbus, Ohio, 1962) p. 11.
3. S. M. OHLBERG, H. R. GOLOB and D. W. STRICKLER, *ibid.* (1962) p. 55.
4. J. W. CAHN, *J. Amer. Ceram. Soc.* **52** (1968) 118.
5. D. R. UHLMANN, *Disc. Faraday Soc. Remarks* **50** (1970) 233.
6. A. H. RAMSDEN, Ph.D. thesis, University of Sheffield, UK (1977).
7. K. NAKAGAWA and T. IZUMITANI, *Phys. Chem. Glasses* **10** (1969) 179.
8. H. HARPER, P. F. JAMES and P. W. McMILLAN, *Disc. Faraday Soc.* **56** (1970) 206.
9. M. TOMOZAWA, *Phys. Chem. Glasses* **14** (1972) 77.
10. K. MATUSITA and M. TASHIRO, *Phys. Chem. Glasses* **15** (1974) 106.
11. P. HAUTOJARVI and V. KOMPPA, *J. Non-Cryst. Sol.* **29** (1978) 365.
12. A. GUINIER, "X-Ray Diffraction", (W. H. Freeman and Co., New York, 1963) p. 327.
13. G. POROD, *Kolloid. Z.* **124** (1951) 83.

14. J. W. CHRISTIAN, "The Theory of Transformations of Metals and Alloys" (Pergamon Press, Oxford and New York, 1969).
15. K. MATUSITA and M. TASHIRO, *J. Non-Cryst. Sol.* **11** (1973) 471.
16. R. T. DE HOFF and F. N. RHINES, *Trans. AIME* **221** (1961) 975.
17. P. F. JAMES, *Phys. Chem. Glasses* **15** (1974) 95.
18. A. F. CRAIEVICH, *ibid.* **16** (1975) 133.
19. J. SLAETS and A. F. CRAIEVICH, *J. Phys. E.* **9** (1976) 739.
20. W. LUZATTI, *Acta Cryst.* **13** (1960) 939.
21. P. F. JAMES, B. SCOTT and P. ARMSTRONG, *Phys. Chem. Glasses* **19** (1978) 24.
22. C. J. R. GONZALES-OLIVER, P. F. JAMES and P. S. JOHNSON, *J. Mater. Sci.* **14** (1979) 1159.
23. K. MATUSITA and M. TASHIRO, *Phys. Chem. Glasses* **14** (1973) 77.

Received 4 August and accepted 4 September 1980.